Design and construction of the lawnmower, an artificial burnt-bridges motor

Suzana Kovacic,[†] Laleh Samii,[†] Paul M.G. Curmi,[‡] Heiner Linke,[§] Martin J. Zuckermann[†] and Nancy R. Forde[†,*]

[†]Department of Physics
Simon Fraser University
8888 University Dr.
Burnaby, BC V5A 1S6
Canada

[‡]School of Physics
University of New South Wales
Sydney, New South Wales 2052
Australia

[§]Nanometer Structure Consortium (nmC@LU) and Division of Solid State Physics
Lund University
Box 118
22100 Lund
Sweden

[*]nforde@sfu.ca

Abstract

Molecular motors of the cell are protein-based, nanoscale machines, which use a variety of strategies to transduce chemical energy into mechanical work in the presence of a large thermal background. The design and construction of artificial molecular motors is one approach to better understand their basic physical principles. Here, we propose the concept of a protein-based, burnt-bridges ratchet, inspired by biological examples. Our concept, the lawnmower, utilizes protease blades to cleave peptide substrates, and uses the asymmetric substrate-product interface arising from productive cleavage to bias subsequent diffusion on the track (lawn). Following experimental screening to select a

protease to act as the motor's blades, we chemically couple trypsin to quantum dots and demonstrate activity of the resulting lawnmower construct in solution. Accompanying Brownian dynamics simulations illustrate the importance for processivity of correct protease density on the quantum dot and spacing of substrates on the track. These results lay the groundwork for future tests of the protein-based lawnmower's motor performance characteristics.

Keywords: molecular motor, protein, quantum dot, trypsin, burnt-bridges

1. Introduction

In its protein-based machines, Nature has provided much inspiration to scientists and engineers about how to extract work from chemical fuel. Molecular motors such as kinesins and dyneins, ATP synthase and polymerases undergo processive motion in an environment rife with thermal fluctuations, coupling their interactions with small-molecule ligands or even protons to directional stepping. This is achieved in great part by exploiting thermally accessed fluctuations and local asymmetry to achieve highly directional stepping.

Recent years have seen a rapid development of micro- and nanoscale devices aimed at achieving directional transport. The field of supramolecular chemistry has developed machines exhibiting (light-)controlled motions on the Ångström scale, while biological polymers have been used in the conception and synthesis of motors capable of directed motion on the nanometer, and even micrometer, length scales.[1-3] The use of nucleic acids to create steppers, driven by base pairing affinities, first led to stepping directed by "fuel" strands, supplied externally in a given temporal order.[4] More recently, the field has seen the development of autonomous DNA-based walkers, whose motion is driven by diffusion and biased via track cleavage.[5-11] The use of proteins as building blocks for *ab initio* designed synthetic motors has not yet seen realized creations. While significant strides forward are being made in the re-engineering of natural motors to produce altered performance,[12-16] the design of new protein-based motors remains in the conceptual phase, with initially proposed concepts controlled by externally gated fuel supply in order to regulate the timescale and directionality of stepping.[2, 17-18]

Because of the near-ubiquity of proteins in natural molecular motors, our work aims to design synthetic protein-based molecular motors constructed from modular building blocks that individually lack motor function.[2] Inspired by the burnt-bridges mechanism proposed for matrix metalloproteases (MMPs),[19-20] the design presented here, dubbed the "lawnmower", uses the cleavage of substrates on a track to rectify diffusion of the motor. The mechanism by which it is designed to operate also bears similarity to the recently demonstrated Par system in *Escherichia coli*, responsible for partitioning DNA during cell division.[21] In this report, we first describe the concept and choice of design components for the lawnmower, then present information on its construction and characterized activity in solution. We follow this up with Brownian dynamics simulations to help predict processivity, and conclude with remarks about the way forward towards demonstrating processive motor activity of the lawnmower.

2. Lawnmower design

2.1 Introduction of concept

The name "lawnmower" relates to the capacity of the molecular motor to cut a lawn of substrate molecules, much like one would mow a lawn of grass using a macro-scale lawnmower (Figure 1). The analogy ends here, however. Whereas a traditional lawnmower is powered by mechanical force, the motion of a nanoscale lawnmower arises from thermal diffusion, and is rectified by the free energy preference to bind uncleaved substrate versus cleaved product sites. Our nanoscale lawnmower is built on a hub, with attached enzymes, such as proteases, serving as its "blades". The lawn consists of a surface displaying substrates for the enzyme. When the lawnmower is placed on the

lawn, productive binding between hub-bound enzymes and substrate molecules produces locally a patch of product on the surface. Decreased binding affinity between enzyme and resulting products allows the blades of the motor to release, permitting diffusion along the lawn to interact with substrate molecules nearby. As the lawnmower processes across the lawn, it leaves an area of product molecules in its wake. Our modeling work on the conceptually related nucleic acid system of the molecular spider suggests that the motion of the lawnmower will be biased and processive if *(i)* the lawnmower has a significantly higher affinity to substrate sites than to product sites, and if *(ii)* at least one blade remains bound to the lawn at all times.[9-10] We note that the lawnmower is designed to work autonomously, with motion biased because of the asymmetry of the substrate-product boundary created through its cleavage activity.

2.2 Choice of hub

The size of the synthetic lawnmower hub is an important consideration in designing the lawnmower, since it relates to the number of blades that can be linked, to the timescale of motor diffusion, and to the range of lawn it can span. Potential candidates include a streptavidin protein, a micron-sized bead, and a nanoscale quantum dot (QD). Since diffusion timescales of any of these over ~10 nm distances are orders of magnitude faster than enzymatic turnover times, we did not rule out any of these options based on this consideration. While streptavidin served as a useful hub for nucleic-acid-based molecular spiders, we were concerned that the limited number (four) of binding sites for blades on each streptavidin hub would result in very low processivity for an enzyme-based lawnmower, given the low affinity of most protein-based enzymes for

their product (in contrast to the higher affinity of deoxyribozyme-based legs of molecular spiders to their oligonucleotide products).[7-8] By contrast, heuristic arguments suggested that on a micron-sized bead hub the large number of enzymes that could simultaneously bind to substrates would result in significant slowing down of the lawnmower, perhaps to levels indistinguishable from noise on an experimentally feasible timescale. A nanoscale QD hub seemed to provide the best compromise, offering enough potential linking sites for blades to increase the binding time of a QD-lawnmower compared to a streptavidin-lawnmower while increasing speed compared to a micron-bead lawnmower. Experimentally, QDs offer significant observation advantages due to their strong fluorescence signal, high emission quantum yields, sharp emission spectra, chemical stability and photostability, allowing ready monitoring of the translocation of a QD-based lawnmower.

A variety of quantum dots with different fluorescence wavelengths and surface chemistries are commercially available. QDs supplied with surface modifications such as carboxyl and amino groups can be utilized as handles to covalently couple a biomolecule of interest to the surface of the QD. From the commercially available QDs, we selected a 16 nm diameter quantum dot with a 605 nm emission wavelength and an amine-derivatized surface to permit covalent coupling of enzymes via appropriate crosslinking reactions (Qdot 605 ITK amino (PEG) quantum dots; Invitrogen). Based on information provided by the manufacturer, these QDs display 10-12 accessible amino groups on the surface of the QD, providing an upper limit for the number of proteases that can be covalently linked to the QD hub.

2.3 Choice of blades

A variety of different enzyme/substrate pairs can be chosen for a lawnmower motor. Analogous to the deoxyribozyme-based molecular spiders, which process on lawns of oligonucleotides,[7-8] a lawnmower could be built using restriction enzymes to process along a one-dimensional DNA track. Alternatively, a lawnmower based on transferases, which could transfer a methyl or phosphate group, could be paired with its appropriate substrate. This option would provide the possibility of a reversible track modification: a phosphatase-based lawnmower could be followed along a track by a kinase-based motor that "replenishes" the track. We chose, however, to focus on a protease-based lawnmower for the practical reason that a wide-variety of proteases and peptide substrates are commercially available, and because of the advantage offered to readily detect enzyme-caused modification of the track. A track composed of fluorogenic substrates can provide a visual readout of lawnmower activity by observing product fluorescence left in the lawnmower's wake (Figure 1).[22] This offers the ability to determine directly the mechanochemical coupling of the motor, as simultaneous observation of the motor's movement (tracking QD position) and the motor's activity (substrate cleavage to generate fluorescent, track-bound products) can be monitored via fluorescence microscopy.

2.4 Choice of linker

Crosslinking reagents of various lengths are commercially available, which offer some control over the span of the blades and the number of blades that can simultaneously bind to a track. By varying the length of the crosslinker between the QD

hub and a protease blade, one can adjust the diffusional search volume of the protease and reduce geometrical and steric constraints between the protease and hub. For ease of construction, the lawnmowers here were constructed using short linkers of length ~ 1 nm. The heterobifunctional chemistry of these sulfo-SMCC linkers (Sulfosuccinimidyl 4-[N-maleimidomethyl] cyclohexane-1-carboxylate, Pierce), which enables attachment at one end to an amine group and at the other to sulfhydryls, is commercially available in chains containing a variable number of polyethylene glycol (PEG) linkers. This permits the modular adaptation of the synthetic approach used here to produce lawnmowers with significantly longer tethers to the blades, whose impact on motor performance could be investigated.[10]

3. Lawnmower Construction

3.1 Experimental screening assays for protease blades

The protease to be used as blades for the lawnmower was selected through an experimental screening process, to ensure that its activity was retained following crosslinking reactions. The sulfo-SMCC linker used to link proteases to the QD hub reacts to link sulfhydryls (on the protease) to amines (on the QD). Thus, we needed to expose or introduce reactive sulfhydryls on the proteases. Two different approaches were tested: either thiol reduction by TCEP (tris[2-carboxyethyl] phosphine) or primary amine thiolation by Traut's reagent (2-iminothiolane). Thiol groups were then reacted with biotin-PEG_2-maleimide and protease activity was monitored at various points in this process.

Protease activity was assayed using a fluorogenic casein derivative as the

substrate (EnzChek Protease Assay Kit red fluorescence, Molecular Probes), and kinetics were measured using a fluorescent plate reader (BioTek Synergy; excitation: 590±20 nm; emission: 645±40 nm). Results from four different proteases are shown in Figure 2. Proteinase K was also tested, and showed a very high activity, but was eliminated due to its non-specific proteolytic activity. Initial cleavage rates over the first eight minutes were determined from the slopes in Figure 2, and for each modification, were compared to the rate of the unmodified control. As shown in Table 1, these tests suggested trypsin (bovine pancreatic, Sigma T8003) as a strong candidate for the protease to use as blades in the lawnmower, due to its retained activity following these chemical modification steps.

Protease	**TCEP**	**TCEP + biotin**	**Traut**	**Traut + biotin**
Trypsin	0.76	1.25	0.73	0.74
Elastase	0.43	0.63	0.96	0.77
Pepsin	0.72	0.94	0.07	0.06
Thrombin	0.51	0.45	0.39	0.11

Table 1. Initial rate of cleavage for each protease following modifications, relative to the rate of the unmodified control.

It is possible, however, that trypsin retains its proteolytic activity following these reactions because it remains unmodified. It is here that the biotinylation serves a second purpose: it allows for indirect confirmation by Western blotting of a successful maleimide-thiol reaction. Figure 3 shows the results of this assay for each of the

proteases tested, for coupling following thiol reduction and via amine thiolation. (Gels were probed with streptavidin-alkaline phosphatase and developed with a chromogenic phosphatase substrate (NBT-BCIP solution, Sigma 72091).) The results confirm that trypsin is a good candidate for a protease-based lawnmower, as it did undergo the desired reactions, producing a good signal in the Western blot for biotin, and as shown in Figure 2, retained proteolytic activity after the biotin-PEG_2 introduction.

3.2 Construction and characterization of lawnmower

Having determined the appropriate components with which to build a prototype lawnmower, the first step in the synthesis was introduction of maleimide moieties on the QD surface by functionalizing 28 pmol of amine-derivatized QDs with 183 nmol of sulfo-SMCC in 20 mM MOPS pH 7.3 buffer (3-(N-Morpholino)propanesulfonic acid, BioXtra Grade, Sigma) in a total volume of 48.5 µL. This buffer was used because it contained less than 0.0005% contamination of copper. Cupric ion concentrations as low as 10 nM can reduce quantum dot fluorescence, while concentrations as little as 50 nM can completely abolish quantum dot fluorescence.[23-24] After 1 hour incubation at room temperature in the dark with rotary mixing, the reaction was quenched with 52 mM β-alanine (Sigma, BioUltra grade), and maleimide-conjugated QDs were purified over a desalting column (Zeba 7K MWCO desalting column, Pierce) that had been pre-equilibrated with 20 mM MOPS pH 7.3. A control sample lacking the crosslinker was similarly treated.

Immediately following preparation of the maleimide-functionalized QD, the lawnmower was constructed by incubating 28 pmol QD with 10 nmol trypsin that had

been treated with Traut's reagent to thiolate primary amine groups on trypsin in a total volume of 100 µL in 20 mM MOPS pH 7.3. (Lawnmowers synthesized using trypsin that had instead been reduced with TCEP to generate free thiols resulted in a significant loss of QD fluorescence. While the cause was not determined, copper contamination in the TCEP reagent is a possible reason.) A control reaction of trypsin and QD lacking maleimide modification was also included. The reaction was incubated at room temperature for 2 hours in the dark with rotary mixing. Samples were concentrated using 50K MWCO centrifugal spin filters (Vivaspin 500, Vivaproducts 1000 rpm, 4 min). Trypsin-conjugated QDs were separated from unconjugated trypsin over Sephacryl S300 (GE Healthcare Life Sciences) size-exclusion gravity columns and eluted with 20 mM MOPS pH 7.3. Peaks were sufficiently resolved to minimize contamination of unconjugated trypsin in the lawnmower fractions (Figure 4).

To identify the successful synthesis of lawnmowers, both QD fluorescence and trypsin activity were monitored in eluate fractions. The trypsin activity of each fraction directly following lawnmower synthesis was monitored using a fluorogenic substrate (EnzChek Protease Assay Kit red fluorescence, Molecular Probes). Background signal from substrate alone (no protease) was subtracted from each measurement, and the slope of the linearly increasing fluorescence intensity versus time was used to assess protease activity. QD fluorescence was monitored at Ex=460/50 nm and Em=595/35 nm. Fractions exhibiting both QD fluorescence and trypsin activity suggest the presence of lawnmowers.

Figure 4 shows the fluorescence signal from QDs and from trypsin cleavage of the fluorogenic substrate, for the collected fractions from reaction and control samples.

As a control, we used a mix of untreated trypsin with unmodified QDs. As expected, in both samples, the QD fluorescence signal was detected in the initial eluted fractions. In the reaction samples, there is a clear increase in protease activity co-eluting with the quantum dots in early fractions, while the control samples show only a low level of peptide hydrolysis signal. We attribute this co-elution of signal to trypsin conjugated to QDs, inferring that successfully conjugated lawnmowers appear most strongly in fractions 4-6 (Figure 4a). Correspondingly, the elution of these larger lawnmowers shifts to earlier fractions from the size-exclusion column compared with unmodified QDs. In both reaction and control, the significant activity peak at later fractions arises from unconjugated trypsin.

We estimated the average number of trypsin molecules conjugated to a QD hub in the active lawnmower fractions by comparing the fluorescence intensity of QDs and rates of cleavage measured for the lawnmower with the intensities of known amounts of QDs and rates of fluorogenic substrate cleavage by known amounts of trypsin (Supplementary Information). For fractions in which lawnmowers were identified to be present, the number of trypsin molecules bound to a QD hub was determined to be about 8, meaning that on average, each lawnmower contains 8 trypsin protease blades, which is comparable to the average number of accessible amino groups on the surface of the quantum dot (10-12).

4. Exploring lawnmower characteristics through simulations

Intuitively, it is easier to characterize directionality on a one-dimensional track of substrates as opposed to a two-dimensional lawn. A 1D lawn limits the direction of

motion of the lawnmower to one of two directions along the track, forwards and backwards, and also decreases the likelihood that the motor will become trapped in a product patch where it is unable to reach substrate and instead becomes detached. Thus, for ease of detecting and characterizing biased motion, initial construction efforts were focused on this 1D realization of a track, tethering fluorogenic peptide substrates for trypsin to a kbp-long DNA backbone.[22]

Geometric arguments suggest that three of the eight protease blades can reach to bind simultaneously to substrates separated by 5 nm on a rigid 1D track. However, a geometric picture provides only what is possible, not necessarily what is probable. To investigate the timescale associated with multiple blades binding to a 1D track, numerical simulations were undertaken.

Brownian dynamics simulations were used to establish time scales of binding as a function of geometric constraints, by calculating when and how many of the proteases attached to one QD can bind to the DNA-attached peptides subsequent to the binding of one initial protease. To represent $N_p = 8$ proteases linked to a common hub, eight polymers modeled by self-avoiding walks were attached to a hub point, where each polymer comprised $N_m = 4$ monomers including the hub point. The monomers are labeled $n = 1, \ldots, N_m$ where $n = 1$ is the hub point, shared by all eight polymers. The first bond of each polymer was 8 nm in length, representing the radius of a QD sphere, and equidistant points on the QD surface were enforced by the imposition of a strong repulsive Coulomb interaction between each of the 2nd monomer ($n = 2$) pairs. Bonds between the next N_m-2 monomers ($n = 2, \ldots, N_m$-1) model the linker attached to the QD; for $N_m = 4$, the linker has one bond of length 0.952 nm. The final bond models the protease, with a length taken

to be 5 nm. The peptide-DNA track was modeled by a one-dimensional lattice with lattice constant d_L. To investigate the role of inter-substrate spacing on motor performance, three values of d_L were used in the simulations: d_L = 5 nm, 10 nm and 20 nm, with the lattice points representing the peptides attached to the DNA backbone. The end monomer ($n = N_m$) can bind to these sites, thus modeling the binding of the protease to the peptides. The binding site has a capture radius r_B, and simulations were run to investigate the influence of this parameter on the efficacy of binding, by considering values for r_B of 0.5 nm, 1 nm and 2 nm. Figure 1 shows a configuration of this simulated lawnmower, and identifies the distances d_L and r_B with the experimental schematic. The Langevin equations of motion for the lawnmower model, the expressions for the interactions used in the simulations and the values of the related parameters are given in the Supplementary Information.

The simulations proceeded as follows. The lawnmower construct was first initialized with one end monomer bound to a binding site on the track. Following this step, any of the other seven end monomers were now able to bind to the track at binding sites other than the one already occupied. As soon as an end monomer entered a binding site, its location was fixed and it could no longer diffuse. The time taken to diffuse to this binding site was recorded as the first-passage time (FPT) for binding of the second protease. The lawnmower underwent continued restricted diffusion, and if a third end monomer (protease) was able to bind, by entering an unoccupied binding site, its FPT for binding was recorded. This procedure continued until the time limit for the run was reached and a new run was initiated.

For each set of parameters, a histogram of observed FPTs was fit to an exponential function to determine the mean FPT. Table 2 gives these values for the binding of a second end monomer (protease), when one end monomer is already bound, as a function of the capture radius, $r_{B,}$ and the DNA lattice spacing, $d_{L.}$ Errors correspond to the 95% confidence level for the exponential fits. 200 independent runs were performed for each set of parameters, each with a cut-off time of 0.92 ms.

r_B \ d_L	5 nm	10 nm	20 nm
0.5 nm	123±6 μs		
1.0 nm	21±5 μs	51±3 μs	112±8 μs
2.0 nm	10±1 μs	12±2 μs	20±1 μs

Table 2. First passage times for the binding of a second end monomer (protease), as a function of the capture radius, $r_{B,}$ and the DNA lattice spacing, $d_{L,}$ determined from 200 independent runs for each entry.

The results in Table 2 show that two proteases can easily bind simultaneously and that the first passage time for this process to occur decreased substantially as either the capture radius increased or the DNA lattice spacing decreased. Binding of a third protease was not observed, even for longer runs with a cut-off time of 23 ms.

These results contrast with the naïve geometric argument that does not take into account entropic flexibility of the system. Even though it is possible that three proteases bind simultaneously to substrates spaced by 5 nm on the track, the Brownian dynamics

simulations show this not to be likely on the timescale of these simulations. Increasing the capture radius facilitated binding of the second protease, but still did not result in binding of a third protease.

As a contrast, we compared the situation when the tether points (n = 2) are allowed to diffuse on the surface of the sphere, achieved by turning off their mutually repulsive "Coulomb" interaction. This would be the situation if, for example, proteases were linked to lipid polar heads in a vesicle rather than to fixed points on the sphere.[25] In this case, our preliminary data showed that three proteases could simultaneously bind within a run time of 0.92 ms. When the radius of the spherical "vesicle" hub was increased to 16nm, four proteases were able to bind within this run time.

5. Discussions and conclusions

Here, we have presented the design and construction of a protein-based, nanoscale motor, dubbed the lawnmower, intended to function as a burnt-bridges ratchet. Our design integrates the function of sterically coupled proteases to convert substrates into products with a one-dimensional presentation of the substrates along a supporting DNA scaffold.[22] This permits the motor-based establishment of local asymmetry in the track, a substrate-product interface, which is key to determining subsequent directionality of motor translocation.[9] By incorporating fluorescence read-out capabilities into both the motor (via the quantum dot hub used to couple the protease blades) and the track (via the signal generated upon cleavage of the fluorogenic substrates), this design enables direct determination of the mechano-chemical coupling of the lawnmower: motion and catalytic

activity proposed to be responsible for the continued biased motion can be observed and correlated.

Our experimental characterization of the lawnmower construct shows that, following covalent chemical coupling to the QD, the trypsin blades retained catalytic activity, and that we were able to couple on average 8 active trypsin molecules to each QD hub. This comes close to saturating the binding capacity of this 16 nm hub (10-12 accessible amino groups), and so the question arises as to whether this geometry presents a sufficient number of blades to achieve processive motion. While geometrically it is possible for three blades to bind simultaneously, our Brownian dynamics simulations suggest that simultaneous binding of more than two proteases to a 1D track is unlikely with the limited linker length employed in this initial design.

The performance of lawnmower as a molecular motor awaits future characterization. Meanwhile, we may speculate about its anticipated performance. Of key concern is processivity: the ability of lawnmower to achieve multiple consecutive cleavage events, thereby biasing its motion, before detaching from the track. Experimental findings by others and our past simulations on the conceptually related molecular spider showed the impact of polyvalency: increasing the number of legs from two to just three resulted in significant enhancements in track residency time, number of cleavages, and distance travelled, while reducing the average speed of spiders on the track.[7, 10] Of course, the processivity of the motor will depend on many experimental factors, including not only the number of blades able to engage the track, but also on the kinetics of binding, cleavage and release of substrate and products.[10] The use of commercially available proteases leaves less control over the latter parameters, while the

former present ample opportunity for tuning. For example, the use of longer linkers makes possible the simultaneous binding of more blades, which may also permit faster translocation along the track.[10] The substrate spacing on the track can be tuned to match the reach of QD-tethered proteases, thereby optimizing the number of blades that can bind for given hub-linker specifications. An additional option is to extend the track from a 1D to a 2D lawn of peptides on a surface, thereby facilitating the binding of more blades, which should increase processivity.[10] The burnt-bridges mechanism has been experimentally demonstrated on a 2D lawn in recent experiments on the Par system of proteins,[21] and has even been inferred from quasi-2D measurements of the nucleic acid spider.[7] Thus, while a 1D presentation of substrate offers the easiest means to characterize and control biased motion, extension to higher dimensions is also possible, and can be explored through future Brownian dynamics simulations and experiments.

In conclusion, the demonstration that our constructed lawnmower is able to cleave substrates presented free in solution opens the door to future experiments designed to assess its performance as a molecular motor. These will permit the assessment of whether the design and construction of the motor produce the expected performance as a burnt-bridges ratchet, and whether this approach is able to achieve an autonomous nanoscale motor made of (non-motor) protein components.

Acknowledgements

All authors acknowledge the Human Frontier Science Program Organization for funding of initial work (HFSP, Grant No. RGP31/2007). Additional support was provided by an NSERC Discovery Grant (NRF), by ComputeCanada and IRMACS through use of

computer facilities (MJZ), and by the Swedish Research Council and nmC@LU (HL). We thank Andrew Wieczorek, Chris Angstmann and members of our motors team for advice and useful discussions.

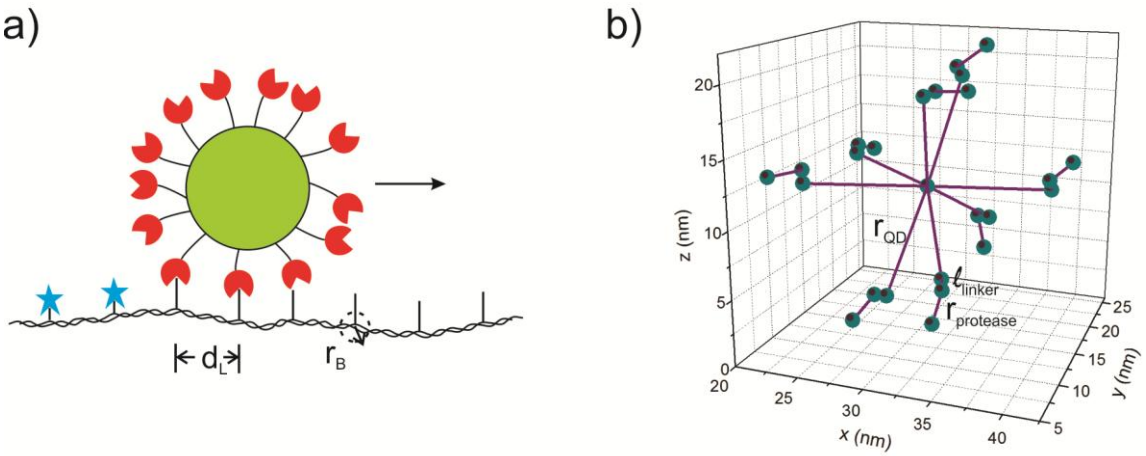

Figure 1 – (a) Schematic of lawnmower. Protease blades are flexibly tethered via covalent linkages to a quantum dot hub. Cleavage of DNA-bound peptides results in their conversion to fluorescent products, thereby creating or maintaining an asymmetric substrate-product boundary in the track. This is designed to bias diffusion towards the substrate region of the track, where there is a free energy preference for binding of proteases (right in this schematic). The use of a fluorescent motor hub and fluorogenic substrates means that motor motility and chemical activity can be simultaneously recorded in experimental assays. d_L and r_B indicate the lattice spacing and capture radius for peptide binding as used in the Brownian dynamics simulations. (b) Snapshot of a lawnmower configuration from the Brownian dynamics simulations. Labelled are the radius of the quantum dot, the length of a linker bond, and the radius of a protease. These simulations used N_m=4 monomers per chain, shown as small spheres in this figure.

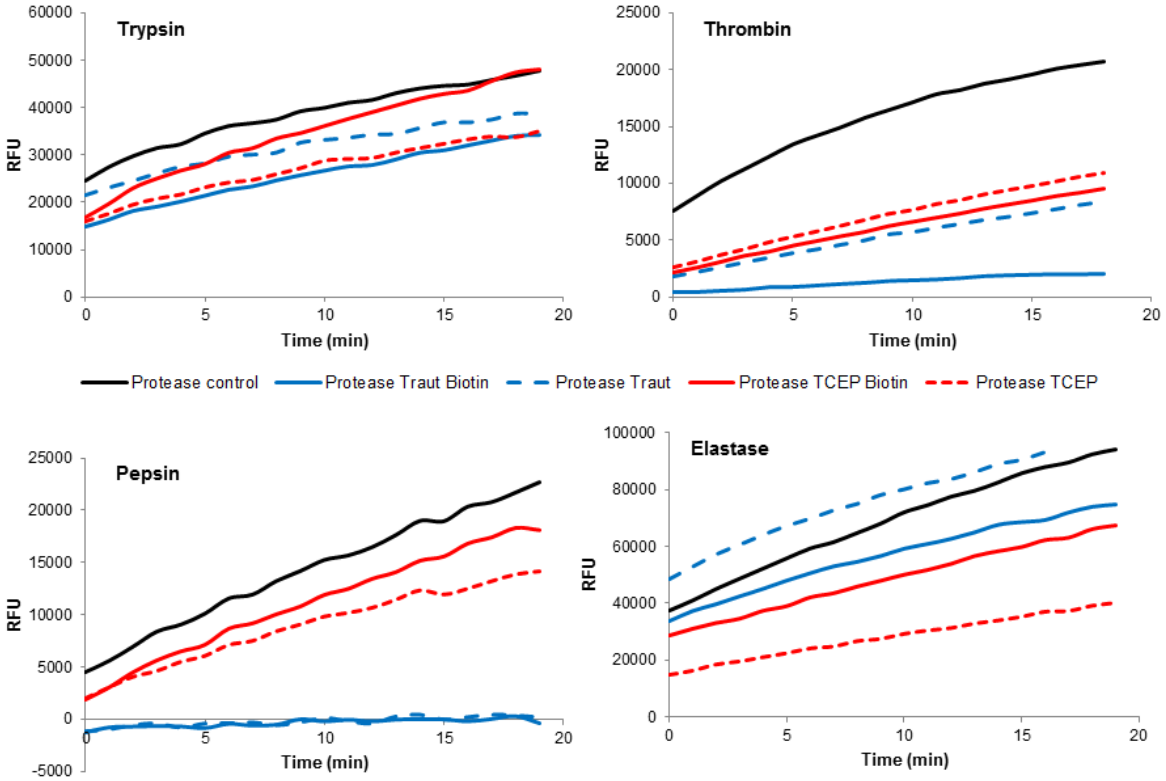

Figure 2 - Activity of proteases after each chemical treatment step toward construction of lawnmower blades investigated using a fluorescence assay. Trypsin showed strong retention of activity after different chemical modifications.

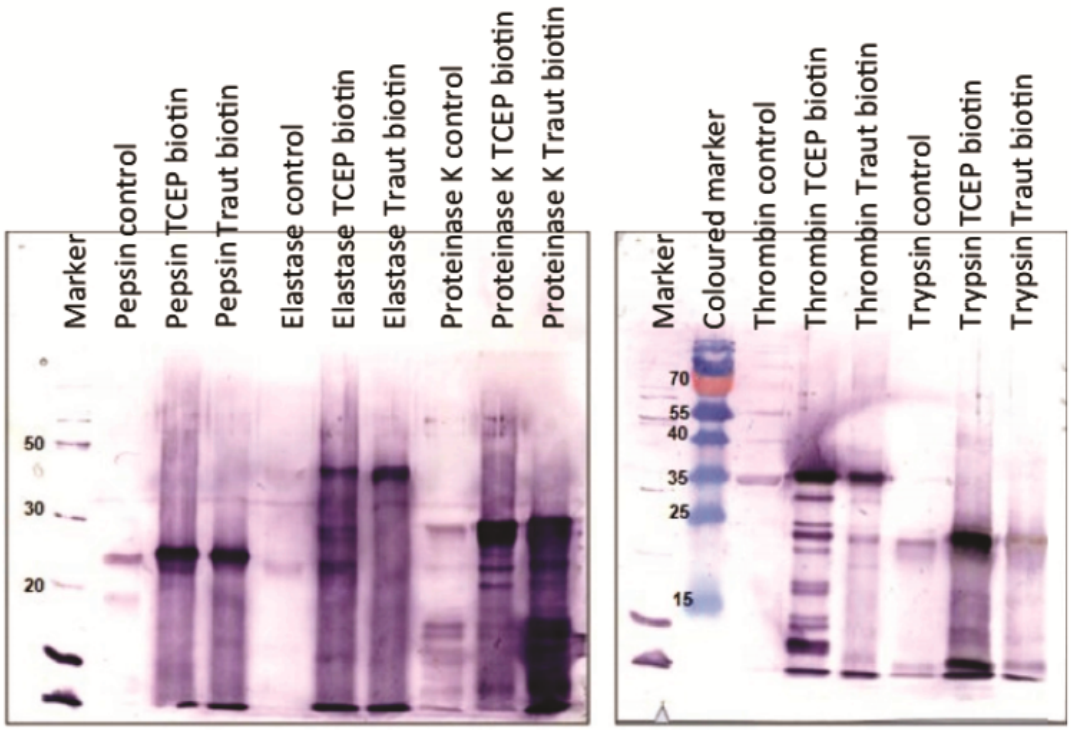

Figure 3 – Western blot analysis of biotinylated TCEP– and Traut– treated proteases. Unbiotinylated proteases serve as negative controls. The intense dark bands in the treated proteases are indications of biotin-PEG_2-maleimide labelling of thiols in these samples.

(a)

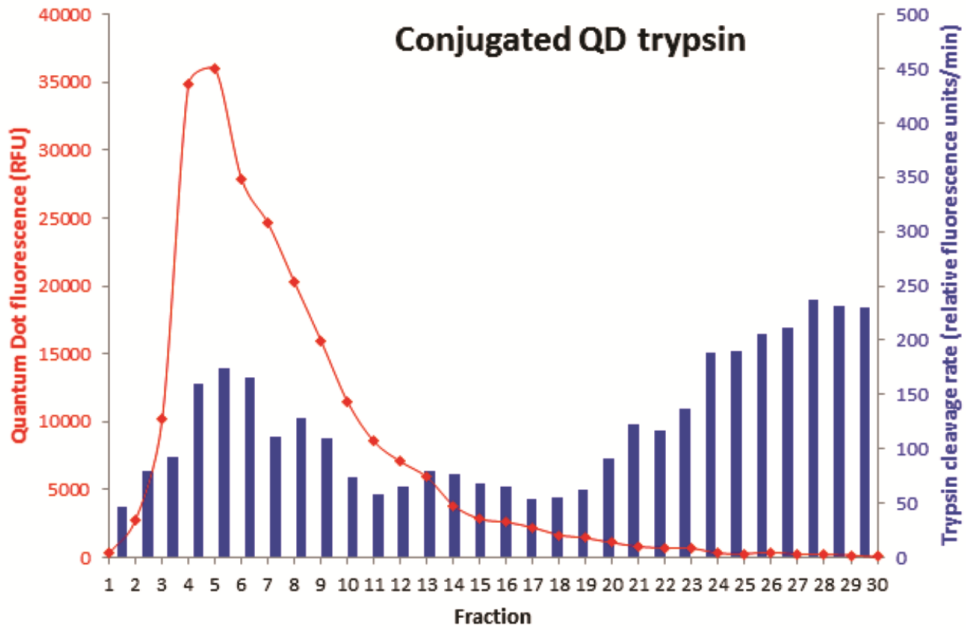

(b)

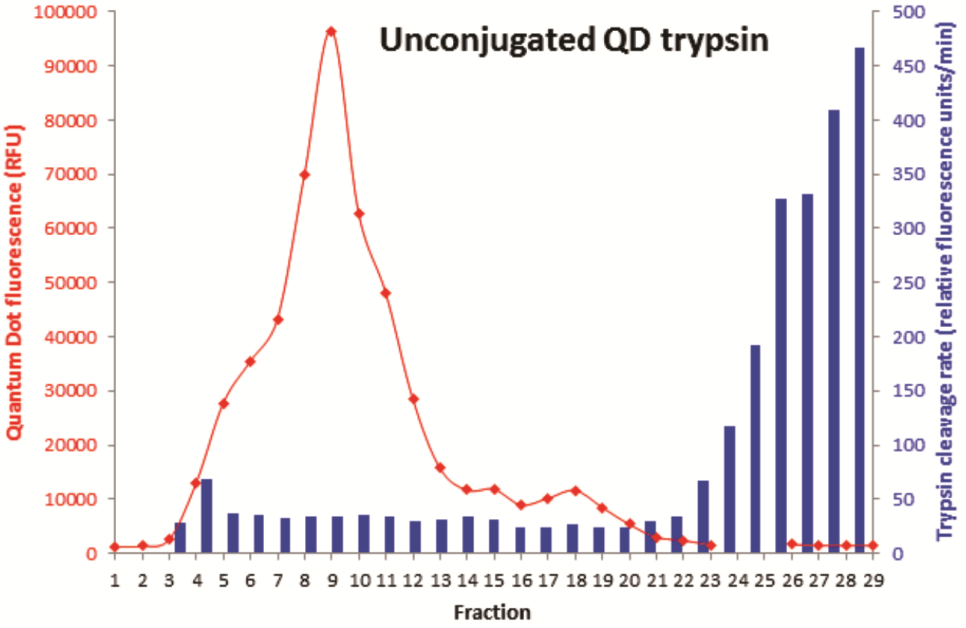

Figure 4 – Size-exclusion chromatogram monitoring the fluorescence signal of both QD (blue points) and from a trypsin kinetic assay (red bars) for the collected fractions from (a) reaction, trypsin-conjugated QD and (b) control, unconjugated trypsin and QD. QD and trypsin-conjugated QD elute earlier from this size-exclusion column while unconjugated trypsin elutes in later fractions.

References

1. von Delius, M.; Leigh, D. A., *Chem. Soc. Rev.* **2011,** *40*, 3656.
2. Bromley, E. H. C.; Kuwada, N. J.; Zuckermann, M. J.; Donadini, R.; Samii, L.; Blab, G. A.; Gemmen, G. J.; Lopez, B. J.; Curmi, P. M. G.; Forde, N. R.; Woolfson, D. N.; Linke, H., *HFSP Journal* **2009,** *3*, 204.
3. Niman, C. S.; Zuckermann, M. J.; Balaz, M.; Tegenfeldt, J. O.; Curmi, P. M. G.; Forde, N. R.; Linke, H., *Nanoscale* **2014**, *6*, 15008.
4. Bath, J.; Turberfield, A. J., *Nature Nanotechnology* **2007,** *2*, 275.
5. Yin, P.; Yan, H.; Daniell, X. G.; Turberfield, A. J.; Reif, J. H., *Angew. Chem.-Int. Edit.* **2004,** *43*, 4906.
6. Bath, J.; Green, S. J.; Turberfield, A. J., *Angewandte Chemie International Edition* **2005,** *44*, 4358.
7. Pei, R.; Taylor, S. K.; Stefanovic, D.; Rudchenko, S.; Mitchell, T. E.; Stojanovic, M. N., *Journal Of The American Chemical Society* **2006,** *128*, 12693.
8. Lund, K.; Manzo, A. J.; Dabby, N.; Michelotti, N.; Johnson-Buck, A.; Nangreave, J.; Taylor, S.; Pei, R.; Stojanovic, M. N.; Walter, N. G.; Winfree, E.; Yan, H., *Nature* **2010,** *465*, 206.
9. Samii, L.; Linke, H.; Zuckermann, M. J.; Forde, N. R., *Physical Review E* **2010,** *81*, 021106.
10. Samii, L.; Blab, G. A.; Bromley, E. H. C.; Linke, H.; Curmi, P. M. G.; Zuckermann, M. J.; Forde, N. R., *Physical Review E* **2011,** *84*, 031111.
11. Wickham, S. F. J.; Endo, M.; Katsuda, Y.; Hidaka, K.; Bath, J.; Sugiyama, H.; Turberfield, A. J., *Nat Nano* **2011,** *6*, 166.
12. Chen, L.; Nakamura, M.; Schindler, T. D.; Parker, D.; Bryant, Z., *Nature Nanotechnology* **2012,** *7*, 252.
13. Goel, A.; Vogel, V., *Nature Nanotechnology* **2008,** *3*, 465.
14. Goodman, B. S.; Derr, N. D.; Reck-Peterson, S. L., *Trends in Cell Biology* **2012,** *22*, 644.
15. Nakamura, M.; Chen, L.; Howes, S. C.; Schindler, T. D.; Nogales, E.; Bryant, Z., *Nature Nanotechnology* **2014,** *9*, 693.
16. Schindler, T. D.; Chen, L.; Lebel, P.; Nakamura, M.; Bryant, Z., *Nature Nanotechnology* **2014,** *9*, 33.
17. Kovacic, S.; Samii, L.; Woolfson, D. N.; Curmi, P. M. G.; Linke, H.; Forde, N. R.; Blab, G. A., *J. Nanomater.* **2012,** *2012*, 109238.
18. Kuwada, N. J.; Zuckermann, M. J.; Bromley, E. H. C.; Sessions, R. B.; Curmi, P. M. G.; Forde, N. R.; Woolfson, D. N.; Linke, H., *Physical Review E* **2011,** *84*, 031922.
19. Saffarian, S.; Collier, I. E.; Marmer, B. L.; Elson, E. L.; Goldberg, G., *Science* **2004,** *306*, 108.
20. Saffarian, S.; Qian, H.; Collier, I.; Elson, E.; Goldberg, G., *Physical Review E (Statistical, Nonlinear, and Soft Matter Physics)* **2006,** *73*, 041909.
21. Vecchiarelli, A. G.; Neuman, K. C.; Mizuuchi, K., *Proceedings of the National Academy of Sciences* **2014,** *111*, 4880.
22. Kovacic, S.; Samii, L.; Lamour, G.; Li, H.; Linke, H.; Bromley, E. H. C.; Woolfson, D. N.; Curmi, P. M. G.; Forde, N. R., *Biomacromolecules* **2014**, *15*, 4065.
23. Xie, H.-Y.; Liang, J.-G.; Zhang, Z.-L.; Liu, Y.; He, Z.-K.; Pang, D.-W., *Spectrochimica Acta Part A: Molecular and Biomolecular Spectroscopy* **2004,** *60*, 2527.

24. Zarkowsky, D.; Lamoreaux, L.; Chattopadhyay, P.; Koup, R. A.; Perfetto, S. P.; Roederer, M., *Cytometry Part A* **2011,** *79A*, 84.
25. Nelson, S. R.; Trybus, K. M.; Warshaw, D. M., *Proceedings of the National Academy of Sciences* **2014,** *111*, E3986.